



VIBRATION BASED HEALTH MONITORING OF HONEYCOMB CORE SANDWICH PANELS USING SUPPORT VECTOR MACHINE

Saurabh Gupta^a, Satish B Satpal^a, Sauvik Banerjee^b and Anirban Guha^{a*}

^aDepartment of Mechanical Engineering, Indian Institute of Technology Bombay, Powai, Mumbai 400076, India

^bDepartment of Civil Engineering, Indian Institute of Technology Bombay, Powai, Mumbai 400076, India

*Email: anirbanguh1@gmail.com

Submitted: Dec. 2, 2015

Accepted: Jan. 16, 2016

Published: Mar. 1, 2016

Abstract- Honeycomb sandwich structures are extensively used in aerospace, aeronautic, marine and automotive industries due to their high strength-to-weight ratios, high energy absorption capability and effective acoustic insulation. Unfortunately, either presence of disbond along the skin-core interface or emergence of disbond due to repeated loading, aging or an intensive load can jeopardize the integrity and safety of the whole structure. The current work presents a new array based technique for health monitoring of these structures using support vector machine (SVM). The proposed technique is first used on simulated mode shape data of the structure and then the technique is validated using experimental mode shape data. The experimental set up has been developed in laboratory and Laser Doppler Vibrometer (LDV) is used to extract the experimental mode shapes. The results have been obtained using both support vector classification and regression analysis and it is found that the former is better at prediction of debond location.

Index terms: Support vector machine, Structural health monitoring, Laser Doppler Vibrometer, Mode Shape Data, Honeycomb core sandwich panel.

I. INTRODUCTION

Honeycomb sandwich panels are made by adhering two high rigidity thin sheets with low density honeycomb core as shown in Figure 1. These panels exhibit very high specific strength and specific stiffness and are widely used in the aerospace industry. The depth of honeycomb core is much higher than the thickness of face sheets. In such a scenario, the transverse shear stiffness is almost completely contributed by the honeycomb core as reported in [1]. The honeycomb core is generally assumed to be a homogeneous material and its equivalent properties are used for the purpose of analysis.

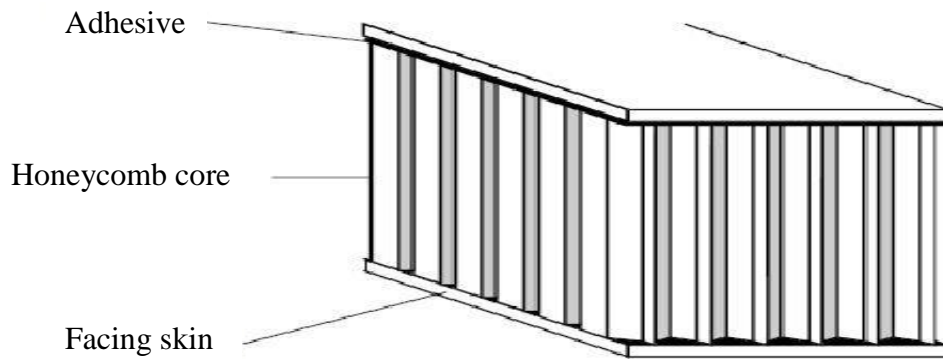


Figure 1. Construction of honeycomb core sandwich panel structure

Bonding of the face sheets to the honeycomb core is a difficult process and the quality of this bonding usually decides the strength of the structure. The most common damage in such structures is debonding between skin and core which occurs either due to manufacturing defects or service loads. Debonded region in a sandwich structure is equivalent to a delamination of composite laminates [2]. Debonding reduces the bending stiffness and resonant frequencies of sandwich structures, and, as the length of debonding increases, the natural frequency decreases and the damping ratio increases. The results indicate that damping can be used as a damage identification feature for honeycomb structures. Figure 2 shows a typical debonding defect in honeycomb structure.

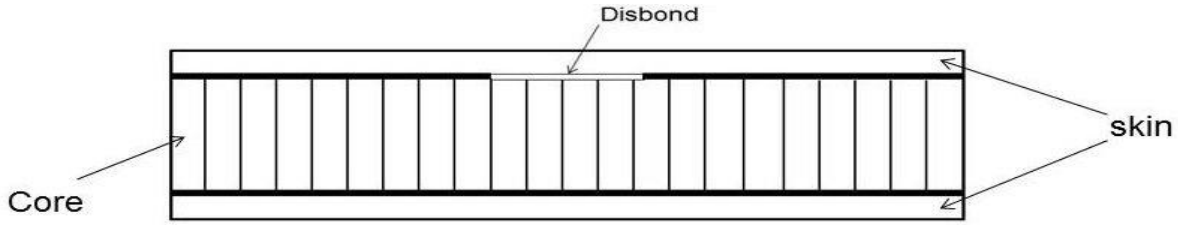


Figure 2. Typical defect in honeycomb structure [3]

A mechanical impedance based method for damage detection in honeycomb core sandwich structure is used by [3] and concluded that for detecting debonding, the test frequency should be lower than the natural frequency of the structure. Delamination is the phenomenon of separation between two composite laminates due to lack of reinforcement in the thickness direction. Delamination occurs under flexural and transverse shear stresses due to quasi-static or dynamic loading. The growth of delamination cracks under subsequent loading leads to a rapid reduction in the mechanical properties and may cause catastrophic failure of the composite structure [4]. The development of the inter-laminar stresses is the primary cause of delamination in laminated fiber composites. Due to the complex nature of laminated composite materials, the onset of damage does not usually lead to ultimate failure, and it is necessary to account for the loss in performance caused by any damage in order to accurately predict the composite material's performance. A technique based on the mode shapes and the variation of the modal damping factors between the undamaged and damaged states of the structure is proposed in [5]. When delamination occurs in a composite structure, energy loss occurs due to friction between the two debonded surfaces. A plane shape function (PSF) is defined for mode r at a node with coordinates (i, j) as given by equation 1.

$$PSF_{i,j}^r = \frac{|x_{i,j}^r|}{\max |x_{i,j}^r|} + \frac{|y_{i,j}^r|}{\max |y_{i,j}^r|} \quad (1)$$

where x and y are two arbitrary mode dependent physical quantities in directions x and y respectively. Strain or displacements can be used for x and y . It is assumed that delamination only leads to increase in damping factor η .

$$\Delta\eta_r^D = \frac{\eta_r^D - \eta_r}{\eta_r} \quad (2)$$

where η = Damping factor

and superscript D stands for damage. Damping Damage Indicator (DaDI) is given by equation 3.

$$DaDI_{i,j} = \frac{\sum_{r=1}^N \left(PSF_{i,j}^r \Delta \eta_r^D \right)}{\sum_{r=1}^N PSF_{i,j}^r} \quad (3)$$

The damage detection techniques can be classified into two categories, model-driven and data-driven techniques. The first technique requires constructing a physical model of a structure (perhaps using FEA) and then comparing the response of damaged and un-damaged structure leading to a decision about its status. In a data-driven technique, the status of the structure is monitored using statistical parameters. Recently, two modeling methods traditionally used in the field of machine learning have been used for SHM. They are Artificial Neural Network (ANN) and Support Vector Machine (SVM). They are different from traditional modeling methods in that the models created using these techniques do not lend themselves to any physical interpretation of the process. They act somewhat like a black box. However, their ability to capture the intricacies of a complex structure is usually superior to the traditional modeling methods. SVM has some advantages over ANN such as:

1. SVM ensures unique and global solution unlike ANN, which may suffer from multiple local minima.
2. SVM can handle high dimensional input data.
3. ANNs are highly prone to over-fitting.

A multi-class pattern classification algorithm of C-support vector machine and the regression algorithm of ϵ -support vector machine to identify the damage location and damage extent, in a continuous girder bridge used in a railway [6]. Banerjee et.al [7] demonstrated the health monitoring of isotropic thin plate structure without base-line signal using a wavelet-based sensing technique. With the help of PZT wafer array of small footprint consisting of a single transmitter and multi-receiver is used. The signals are recorded first for undamaged plate and compared with theoretical model in order to tune an appropriate guided wave. The types of defect attempted to indentify are cracks and loose rivet holes with damage index algorithm and depending on the

value of damage index the damages have been quantified. Generating and monitoring lamb waves using PZT transducers and fiber optic sensors to monitor health of aerospace structure is demonstrated in [8]. This proposed hybrid approach together with an in-house developed algorithm is explored to detect and localize through thickness damage and surface damage located on backside of the plate. Cross-correlation of forward and backward propagating wavefields in composite structures using flexural wave signals is studied in [9]. The proposed approach is verified by conducting experiments using laser Doppler vibrometer to receive the scattered wave signals along a linear array. SHM of aerospace structures based on dynamic strain measurements using SVM classification has been studied in [10]. The feature space has been reduced using Independent Component Analysis (ICA). The results show that SVMs using nonlinear kernel is a reliable and consistent pattern recognition scheme for damage diagnosis. The use of SVM for prediction of fault in power systems has been demonstrated [11]. They used support vector classification to predict the damage location. The inputs used for SVM model are power and voltage values. A demonstration of damage detection process in civil structures using SVM classifiers and wavelet is given in [12]. They found that the SVM was a robust classifier in presence of noise whereas wavelet-based compression gracefully degrades its classification accuracy. A SVM classifier for fault diagnosis of the broken rotor bars of a squirrel-cage induction motor is explored in [13]. They used the spectral information of the motor current, voltage and shaft field as selected features from the input vector applied to the support vector machine. Recently, SVM (regression) based approach to locate the damage in an aluminium beam using mode shape data corresponding to first natural frequency has been proposed in [14]. The technique has been validated using experimental mode shape data of the beam. Thus, literature shows promising results in SHM using both support vector classification and regression, the latter being more common. However, a comparative study of these two techniques in a complex structure like a honeycomb core sandwich panel has not been attempted. This paper attempts to do this using only the first mode shape displacement data. The motivation for using the first mode shape displacement data is that this would lead to less pre-processing of the data compared to other techniques. A cantilever boundary condition has been chosen for ease of conducting the experiment. Initially, FEA analysis of honeycomb panel is done using Abaqus® and mode shape data is extracted at the first natural frequency. Thereafter, experimental mode

shape data has been obtained using Laser Doppler Vibrometer (LDV) and has been used for validation of the proposed technique.

II. FINITE ELEMENT MODELING AND ANALYSIS

The honeycomb core is modeled in Abaqus[®] 6.10. The properties used for modeling honeycomb panel are listed in table 1. Two regions, intact and debond, were defined in the plate's FE model as shown Figure 3. The surfaces have been created on each face sheet and core, then tie constraint is applied except for the debond region in order to create debond of the required area.

Table 1.Honeycomb panel parameters

Parameters	Value
Length of panel	250mm
Width of panel	250mm
Element size	5mm
Element type	S4R shell
Face Sheet-Aluminum (AA 2024 T3)	
Thickness	0.25mm
Young's Modulus	70GPa
Poisson's Ratio	0.33
Density	2800Kg/mm ³
Shear Modulus	27GPa
Honeycomb Core-Aluminum (Low density) Core 3/16-5056-0.0007)	
Thickness	25mm
Density	32Kg/m ³
Young's Modulus	1KPa, 1Kpa (Ex , Ey)
Shear Modulus	1KPa,0.185GPa,0.89Gpa (Gxy, Gyz, Gzx)

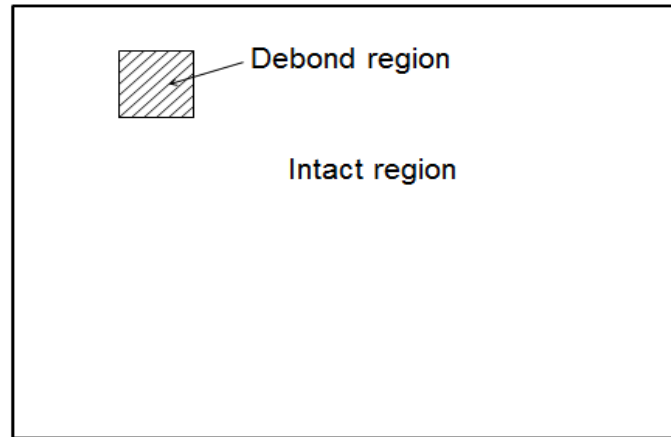


Figure 3. Debond modeling approach used in Abaqus[®] 6.10

The displacement values of the plate at first natural frequency have been measured at various points which are marked in red color along X and Y direction as shown in Figure 4.

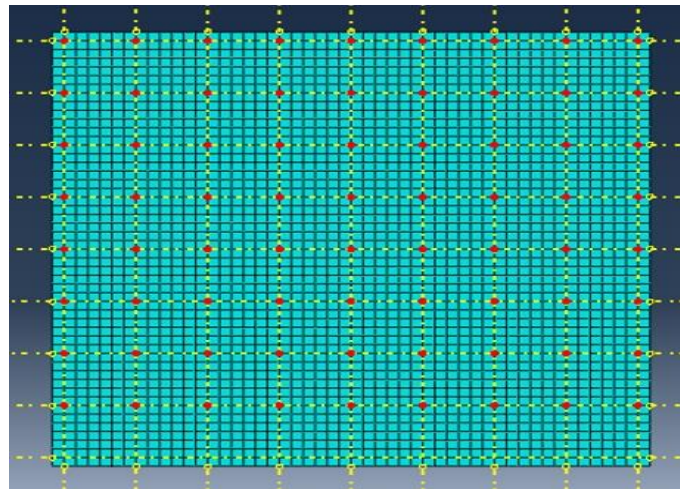


Figure 4. Data measurement points shown in red color

III. OVERVIEW OF SUPPORT VECTOR MACHINE (SVM)

SVM is an algorithm drawn from pattern recognition background. Initially it was developed for classification problem and eventually it has been applied for regression analysis. In this section a brief overview of SVM is given.

a. SVM for classification

Consider the problem of binary classification. Training data are given as

$$(x_1, y_1), (x_2, y_2), \dots, (x_l, y_l), x \in \mathfrak{R}^n, y \in \{+1, -1\} \quad (1)$$

For simplicity consider a 2-dimensional input space i.e., $x \in \mathfrak{R}^2$ which is linearly separable in +1 and -1 classes with a hyperplane say H

$$(w^T \cdot x + b) = 0 \quad (2)$$

where, x is input space, w is weight vector and b is bias term.

In Figure 5 the separating hyperplane H , is shown in dashed line and the planes shown in thick line are called margins. Let them be called $H1$ and $H2$ in class 1 and 2 respectively and the distance between them is called as margin, M .

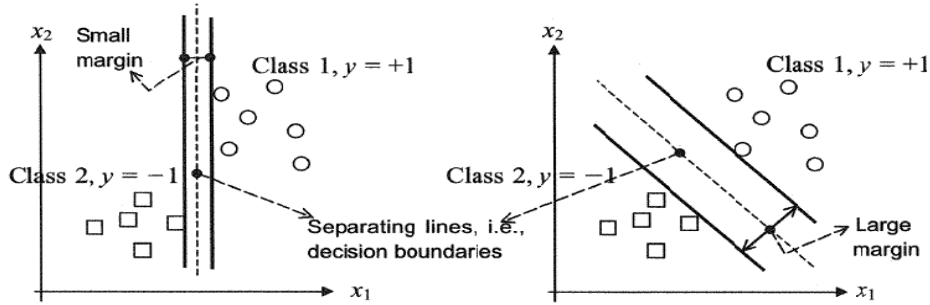


Figure 5. Two out of many separating lines: *right*, a good one with a large margin, and *left*, a less acceptable one with a small margin

They pass through the closest points in both classes. The closest points are called the support vectors. There can be infinite hyper planes which separate the given data, but the best classifier is one that maximizes the margin which is given by

$$M = \frac{2}{\|w\|} \quad (3)$$

Maximizing margin given by equation (3) means minimizing the norm of the weight vector w and minimization of norm $\|w\| = \sqrt{w^T w} = \sqrt{w_1^2 + w_2^2 + \dots + w_n^2}$ equals a minimization of

$w^T w = \sum_{i=1}^n w_i^2 = w_1^2 + w_2^2 + \dots + w_n^2$. Hence, the problem becomes

$$\text{Minimize} \quad \frac{1}{2} w^T w \quad (4)$$

$$\text{Subject to } y_i [w^T \cdot x + b] \geq 1, \quad i=1, l$$

where l denotes the number of training data points.

This is a classic quadratic optimization problem with inequality constraints. Such an optimization problem is solved by Lagrangian method.

$$L_p(w, b, \alpha) = \frac{1}{2} w^T w - \sum_{i=1}^l \alpha_i \{y_i [w^T \cdot x + b] - 1\} \quad (5)$$

where, α_i are the Lagrangian multipliers.

This problem can be solved in primal space (space of w and b) or in dual space (space of Lagrange multipliers α_i). The later approach is implemented here. To do so, Karush-Kuhn Tucker (KKT) conditions are used such that the derivatives of Lagrangian L_p with respect to primal variables should vanish which leads to,

$$\frac{\partial L_p}{\partial w} = 0 \quad \text{i.e., } w = \sum_{i=1}^l \alpha_i y_i x_i \quad (6)$$

$$\frac{\partial L_p}{\partial b} = 0 \quad \text{i.e., } \sum_{i=1}^l \alpha_i y_i = 0 \quad (7)$$

$$\alpha_i \{y_i [w \cdot x + b] - 1\} = 0 \quad i=1, l \quad (8)$$

Substituting equations (6, 7) in equation (5) we get the Lagrangian formulation in dual variable as given below

$$L_d(\alpha) = \sum_{i=1}^l \alpha_i - \frac{1}{2} \sum_{i,j=1}^l y_i y_j \alpha_i \alpha_j x_i^T x_j \quad (9)$$

In order to find the solution, equation (9) need to be maximized with respect to non-negative α_i and with the constraints

$$\alpha_i \geq 0 \quad i=1, l \quad (10a)$$

$$\sum_{i=1}^l \alpha_i y_i = 0 \quad (10b)$$

In matrix notation the above standard optimization problem can be expressed and formulated as given below

$$\text{Maximize } L_d(\alpha) = -0.5 \alpha^T H \alpha + f^T \alpha \quad (11a)$$

$$\text{Subject to } y^T \alpha = 0 \quad (11b)$$

$$\alpha_i \geq 0 \quad i=1, l \quad (11c)$$

where, $\alpha = [\alpha_1, \alpha_2 \cdots \cdots \alpha_l]^T$, $H = y_i y_j x_i^T x_j$ and f is an $(l, 1)$ unit vector. After obtaining solution α from the above optimization problem, the weight vector w and bias b are calculated as

$$w = \sum_{i=1}^l \alpha_i y_i x_i \quad (12a)$$

$$b = \frac{1}{N_{sv}} \left(\sum (y_s - x_s^T w) \right), \quad s = 1, N_{sv} \quad (12b)$$

Where, N_{sv} denotes the number of support vectors. Training input data having non-zero Lagrange multipliers are called support vectors. Having calculated the value of weight vector and bias term, final expression for separating hyperplane is written as

$$f(x) = \sum_{i=1}^l y_i \alpha_i x_i^T x_i + b \quad (13)$$

In case the two classes are not completely separable, positive slack parameters ξ_i are introduced into the equations of the margins. This is referred as soft margins. The modified equations of margins are

$$y_i [w^T x + b] \geq 1 - \xi_i, \quad i=1, l \quad (14)$$

$$\alpha_i \leq C \quad (15)$$

The primal form of the Lagrangian for the non-separable case is:

$$L_p = \frac{1}{2} \|w\|^2 + C \sum_{i=1}^l \xi_i - \sum_{i=1}^l \alpha_i \{y_i [w^T x + b] - 1 + \xi_i\} - \sum \mu_i \xi_i \quad (16)$$

where μ_i are Lagrangian parameters to force $\xi_i \geq 0$.

In reality, most classes are overlapped and the genuine separation lines are nonlinear hypersurfaces. SVM can create a nonlinear decision hypersurface which will be able to classify nonlinearly separable data. The idea is to map the input vector x to a higher dimension vector z using a mapping vector function vector Φ . The dot product $(x_i \cdot x_j)$ will change to $(\phi_i \cdot \phi_j)$. But the computation can be very costly depending on the dimension of vector z . The best way to address the problem is to introduce a function K such that

$$K(x_i \cdot x_j) = (\phi_i \cdot \phi_j) \quad (17)$$

The function K is called kernel function. The same approach with some modifications is implemented to formulate SVM to perform regression analysis [15].

IV. PREDICTION OF DEBOND LOCATION USING SIMULATION DATA

a. Procedure

A total of 17 samples having single damage (debond) of $30 \times 30 \text{ mm}^2$ area at particular locations have been modeled and the corresponding first mode shape data is obtained. The feature vector for SVM is prepared using mode shape displacement data. Out of 17, mode shape data of 13 damaged honeycomb panels have been used as training set and 4 damaged sample's mode shape data is used as test set. The locations of damages used for the training set are shown in Figure 5 and those for the test set as shown in Figure 6. The training set should be prepared in such a way that it includes information from all regions of the structure, therefore the mode shape data associated with the debond locations from all the region of honeycomb panel is included in the training set. Prediction of debond location is carried out in two ways, SV classification and SV regression. In case of classification the debond locations have been assigned class numbers. For example, panel having damage no 1 (S1) lies in horizontal zone C4 and C5 and in vertical zones V4 and V5. Therefore, the training output for the feature vector associated with these zones are assigned as class 1 and rest as class -1. Table 2 demonstrates the output of the training set for all the debond locations considered in the study. In case of SV regression analysis, the outputs of the training set have been assigned X and Y co-ordinates of the debond location. Therefore, SV regression analysis involves two steps (prediction of X and Y co-ordinate independently) in order to locate debond. A Matlab[®] toolbox developed by Gunn [16] is used to carry out the SV analysis.

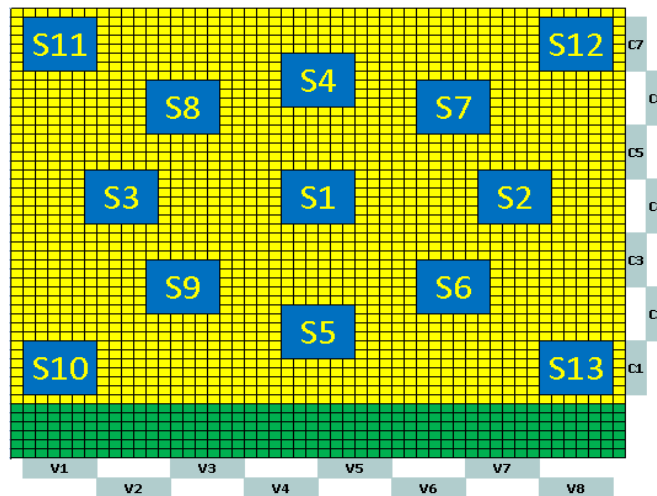


Figure 5. Debond locations associated with training set

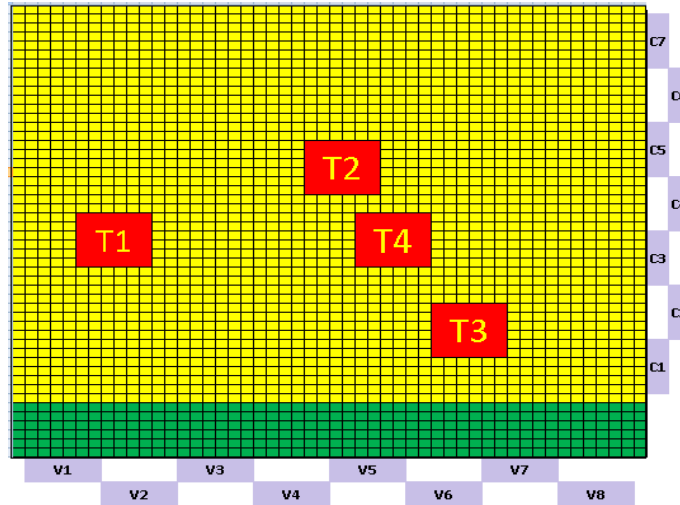


Figure 6. Debond locations associated with test set

Table 2. Training output vectors for seven horizontal and eight vertical zones

Damage No. / Class	1	2	3	4	5	6	7	8	9	10	11	12	13
C1	-1	-1	-1	-1	1	-1	-1	-1	-1	1	-1	-1	1
C2	-1	-1	-1	-1	1	1	-1	-1	1	1	-1	-1	1
C3	-1	-1	-1	-1	-1	1	-1	-1	1	-1	-1	-1	-1
C4	1	1	1	-1	-1	-1	-1	-1	-1	-1	-1	-1	-1
C5	1	1	1	-1	-1	-1	1	1	-1	-1	-1	-1	-1
C6	-1	-1	-1	1	-1	-1	1	1	-1	-1	1	1	-1
C7	-1	-1	-1	1	-1	-1	-1	-1	-1	-1	1	1	-1
V1	-1	-1	1	-1	-1	-1	-1	-1	-1	1	1	-1	-1
V2	-1	-1	1	-1	-1	-1	-1	1	1	1	1	-1	-1
V3	-1	-1	-1	-1	-1	-1	-1	1	1	-1	-1	-1	-1
V4	1	-1	-1	1	1	-1	-1	-1	-1	-1	-1	-1	-1
V5	1	-1	-1	1	1	-1	-1	-1	-1	-1	-1	-1	-1
V6	-1	-1	-1	-1	-1	1	1	-1	-1	-1	-1	-1	-1
V7	-1	1	-1	-1	-1	1	1	-1	-1	-1	-1	1	1
V8	-1	1	-1	-1	-1	-1	-1	-1	-1	-1	-1	1	1

b. Results

The results obtained after prediction of the debond location by SV classification have been presented in tabular form as shown in table 3. The debond location numbers 2 and 3 have been predicted accurately but there is a considerable error in prediction of X any Y co-ordinates of

debond locations 1 and 4. The last two columns represent percentage error in prediction of X and Y co-ordinate respectively which are normalized with the length of the panel. The predictions are reasonably accurate except for X co-ordinate of debond region T1 and Y co-ordinate of debond region T4.

Table 3. Results for Honeycomb panel using SV classification

Test Damage	Predicted		Actual		Absolute Error X	Absolute Error Y	Percentage Error in X	Percentage Error in Y
	zone C	zone V	zone C	zone V				
T1	5	2	4	2	30	0	12	0
T2	5	4	5	4	0	0	0	0
T3	1	7	1	7	0	0	0	0
T4	4	1	4	5	0	120	0	48

With help of same data set (first mode shape displacements), the debond locations have next been predicted using SV regression analysis. The results have been reported in table 4. The last two columns show the percentage error which have been normalized with length of the panel. In this case, prediction of X co-ordinate is better as compared to Y co-ordinate.

Table 4. Results for Honeycomb panel using SV regression based on simulation data

Test Damage	Predicted		Actual		Absolute Error in X	Absolute Error in Y	Percentage Error in X	Percentage Error in Y
	X	Y	X	Y				
T1	85.13	121.55	40	120	45.13	1.55	18.052	0.62
T2	125.78	143.6	130	160	4.22	16.4	1.688	6.56
T3	174.37	114.49	180	70	5.63	44.49	2.252	17.796
T4	140.71	152.14	150	120	9.29	32.14	3.716	12.856

V. VALIDATION OF THE PROPOSED TECHNIQUE

In this section, the proposed technique has been validated using experimental mode shape data. Four specimens of honeycomb core sandwich panels were fabricated at ISRO Satellite Centre,

Bangalore. The material and properties for the panel are mentioned in table 1. The debond in all the four specimens was created during fabrication at known locations. All the four panels were made out of a single panel and later they were cut to four pieces. Three holes were provided in each panel to hold them as cantilever during vibration test.

Table 5. Technical Specifications of PSV-400-3D Vibrometer

Parameter	Detail
Model	PSV-400-3D
Frequency Range	Up to 25000 Hz
Angular Resolution	Less than 0.002°
Scanning Range	±20° about X,Y
Scan Speed	30 points/s(typical) (can be varied)
Working distance	0.35 m to 5 m

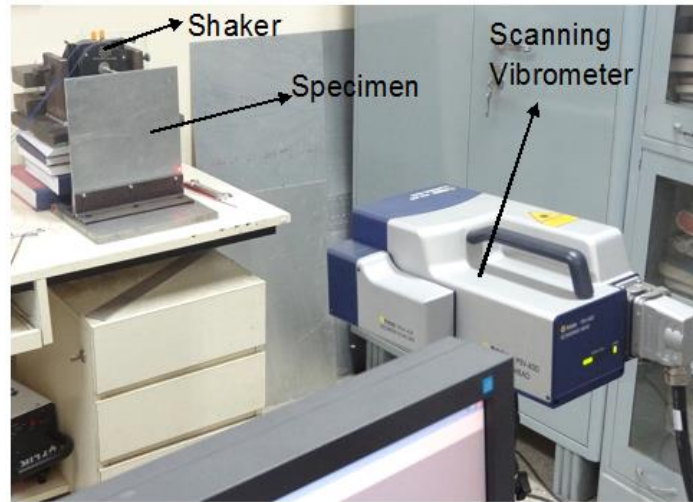


Figure 7. Experimental Setup

A fixture for holding honeycomb panels and aluminum plates is designed. The fabrication is done at ISRO Satellite Centre. The specimens were given a square wave excitation using a vibration shaker. The displacements for the first mode shape are measured using Polytec PSV-400-3D scanning vibrometer. The specifications of vibrometer are listed in table 5.

The complete setup is shown in Figure 7. Vibration test is performed at National Aerospace Laboratory (NAL), Bangalore. Square wave excitation is used for the vibration test. The

displacements are measured at predefined locations. A sweep of frequency in the range of the natural frequency of the structure is made. The first mode shape is identified from the first peak in the displacements over the frequency range scanned.

The experimental mode shape displacement data of the honeycomb core panel is used to predict the debond location. The procedure for preparation of the feature vector is same as that for the simulated data. Table 6 demonstrates the prediction results obtained using SV classification. It is seen that the experimental mode shape data gives higher error in predicting Y co-ordinates as compared to the X co-ordinates of the debond regions.

A similar exercise was conducted using the experimental mode shape data with SV regression analysis and the results have been summarized in table 7. The predictions of X and Y co-ordinates of the debond region are poor while using SV regression analysis as compared to SV classification analysis. The overall location prediction is worse than what was possible from simulated data. This was expected since the boundary conditions of the experiment, though setup with care cannot be expected to mimic the exact conditions of the simulation.

Table 6. Results for Honeycomb panel using SV classification based on experimental data

Test Damage	Predicted		Actual		Absolute Error in X (mm)	Absolute Error in Y (mm)	Percentage Error in X normalized	Percentage Error in Y normalized
	zone C	zone V	zone C	zone V				
T1	5	3	4	2	30	30	12	12
T2	4	4	4	4	0	0	0	0
T3	2	2	2	6	0	120	0	48
T4	2	1	3	5	30	120	12	48

Table 7. Results for Honeycomb panel using SV regression based on experimental data

Test Damage	Predicted		Actual		Absolute Error in X (mm)	Absolute Error in Y (mm)	Percentage Error in X normalized	Percentage Error in Y normalized
	X	Y	X	Y				
T1	28	21.9	40	120	12	98.1	4.8	39.24

T2	24.21	19.51	130	160	105.79	140.49	42.316	56.196
T3	27.63	21.83	180	70	152.37	48.17	60.948	19.268
T4	27.24	81.63	150	120	122.76	38.37	49.104	15.348

The error predicted for the X and Y co-ordinates have been represented graphically in figures (8 and 9) using SV classification and regression respectively as shown below.

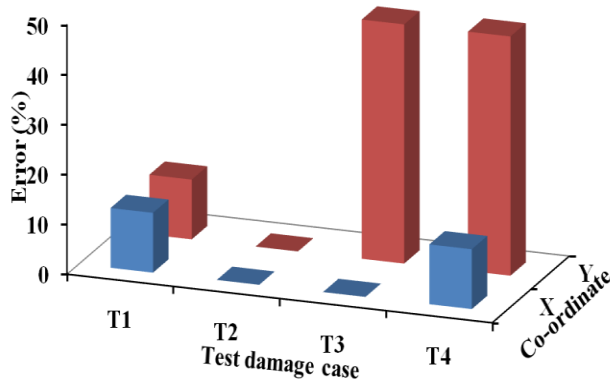


Figure 8. Error prediction using SV Classification

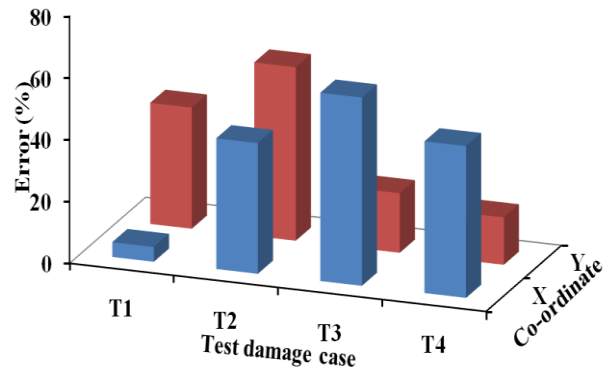


Figure 9. Error prediction using SV regression

ACKNOWLEDGMENT

Authors would like to specially thank Shri S. Kalyana Sundaram, Principal Scientist, National Aerospace Laboratories, Bangalore for making his facility available to conduct vibration test. Authors would like to sincerely thank Structures Group and Facilities Group of ISRO Satellite Centre for the fabrication of Honeycomb Core Sandwich Panels and fixture for experimental setup.

REFERENCES

[1] H.Meifeng and H.Wenbin, "A study on composite honeycomb sandwich panel", *Materials and design*, Vol. 29, 2008, pp. 709-713.

- [2] Y.K.Hyeung and H.Woonbong, “Effect of debonding on natural frequencies and frequency response functions of honeycomb sandwich beams”, *Composite structures*, Vol.55, 2002, pp. 51-62.
- [3] M.K.Lim, S.C.Low, L.Jiang and K.M.Liew, “Dynamic characteristics of disbands in honeycomb structures”, *Engineering structures*, Vol. 17, 1995, pp. 27–38.
- [4] K.B.Su, “Delamination resistance of stitched thermoplastic matrix composite laminates”, *Advances in thermoplastic matrix composite materials*, Vol. 1044, 1989, pp. 279-300.
- [5] D.Montalvao, A.M.R.Ribeeiro, J.Duarte-Silva, “A method for the localization of damage in CFRP plate using damping”, *Mechanical systems and signal processing*, Vol. 23, 2009, pp. 1846-1854.
- [6] B.Sauvik, M.Debdatta and M.S.Shaik, “wavlet-based active sensing for health monitoring of plate structures using baseline free ultrasonic guided wave signals”, *International journal on smart sensing and intelligent systems*, vol. 6, no. 4, 2013, pp. 1435-1455.
- [7] S.Deshan, F.U.Chunyu, LI. Qiao LI, “Experimental investigation of damage identification for continuous railway bridges”, *Journal of Modern Transportation*, Vol. 20, No.1, 2012, pp. 1-9.
- [8] B.Darun, M.Marcias, R.Bruno and Y.Marko, “ A Hybrid Structural Health Monitoring System for the Detection and Localization of Damage in Composite Structures”, *Journal of Sensors*, 2014, vol. 2014, doi:10.1155/2014/109403.
- [9] H.Jiaze and Y. Fuh-Gwo , “Damage identification for composite structures using a cross-correlation reverse-time migration technique”, *Structural Health Monitoring*, 2015, vol. 14 No. 6, pp. 558-570.
- [10] T.H.Loutas, A.O.Panop, D.Roulias and V.Kostopoulos, “Intelligent health monitoring of aerospace composite structures based on dynamic strain measurements”, *Expert systems with application*, Vol. 39, 2012, pp. 8412-8422.
- [11] S.K.Kumar, T.Jayabarathi and S.Naveen, “Fault identification and location in distribution systems using support vector machines”, *European Journal of Scientific Research*, Vol. 51, 2011, pp. 53-60.
- [12] B. Ahmet, S. K.Ambuj, S.Peter, F.Tony, J.Hector, Y.Linjun and E.Ahmed, “Real-time nondestructive structural health monitoring using support vector machines and wavelets”, *Proc.*

SPIE 5770, Advanced Sensor Technologies for Nondestructive Evaluation and Structural Health Monitoring, 2005, doi:10.1117/12.597685.

[13] K. Jaroslaw and S.Osowski, "Support vector machine for fault diagnosis of the broken rotor bars of squirrel-cage induction motor", *Neural Computation & Application*, Vol. 19, 2010, 557-564.

[14] S. Satish, G.Anirban and B.Sauvik, "Damage identification in aluminium beams using support vector machine: Numerical and Experimental studies", *Struct. Control Health Monit.*, 2015, doi:10.1002/stc.1773.

[15] A.J.Smola and B.Scholkopf, "A tutorial on support vector regression", *Statistics and Computing*, Vol. 14, 2004, No. 3, pp 199-222.

[16] S.R. Gunn, "Support Vector Machines for Classification and Regression," *technical report, School of Electronics and Computer Science*, Univ. of Southampton, Southampton, U.K., 1998.